Graphene oxide-gold nanoparticles hybrids-based surface plasmon resonance for sensitive detection of microRNA

Qing Wang, Qing Li, Xiaohai Yang, Kemin Wang, Shasha Du, Hua Zhang, Yajie Nie

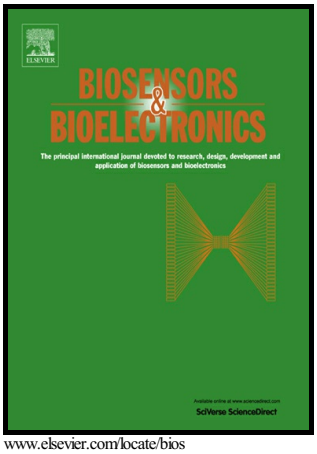

www.elsevier.com/locate/bios

PII: S0956-5663(15)30551-0
DOI: http://dx.doi.org/10.1016/j.bios.2015.10.091
Reference: BIOS8127

To appear in: *Biosensors and Bioelectronic*

Received date: 3 October 2015
Revised date: 28 October 2015
Accepted date: 30 October 2015

Cite this article as: Qing Wang, Qing Li, Xiaohai Yang, Kemin Wang, Shasha Du, Hua Zhang and Yajie Nie, Graphene oxide-gold nanoparticles hybrids-based surface plasmon resonance for sensitive detection of microRNA, *Biosensors and Bioelectronic,* http://dx.doi.org/10.1016/j.bios.2015.10.091

Graphene oxide-gold nanoparticles hybrids-based surface plasmon resonance for sensitive detection of microRNA

Qing Wang, Qing Li, Xiaohai Yang, Kemin Wang*, Shasha Du, Hua Zhang, Yajie Nie

State Key Laboratory of Chemo/Biosensing and Chemometrics, College of Chemistry and Chemical Engineering, Key Laboratory for Bio-Nanotechnology and Molecular Engineering of Hunan Province, Hunan University, Changsha 410082, China

* E-mail address: kmwang@hnu.edu.cn; Tel/Fax: +86-731-88821566.

Abstract

In this study, a simple and sensitive surface plasmon resonance (SPR) biosensor for miRNA detection was developed using graphene oxide-gold nanoparticles (GO-AuNPs) hybrids as signal amplification element. Taking advantage of the GO-AuNPs hybrids and their enhanced performance in SPR biosensors, the detection of miRNA was carried out in only two steps. Firstly, the thiolated capture DNA probe with a short complete complementary sequence was immobilized on the Au film surface to recognize the part sequence of target miRNA. Subsequently, the assistant DNA-linked GO-AuNPs hybrids were employed to bind the other section of the target. It was found that the developed SPR biosensor was able to achieve a detection limit as low as 1 fM. Moreover, the method showed excellent ability to discriminate differences among miRNA-200 family members. Notably, human miRNA from cancer cells could also be detected, and the results were in excellent agreement with the ones obtained using qRT-PCR. On the basis of these findings, we believe that this method has great potential for quantitative detection of miRNA in biomedical

research and early clinical diagnostics.

Keywords: Surface plasmon resonance; MicroRNA; Graphene oxide-gold nanoparticles hybrids.

Introduction

MicroRNA (miRNA) is a short endogenous, noncoding ribonucleic acid molecule that is frequently dysregulated in various types of human cancers (He and Hannon, 2004). Increasing evidences have suggested that a large number of genetic diseases are associated with miRNAs dysregulation, and miRNA expressions are closely associated with the pathogenesis of most human malignancies (Calin and Croce, 2006; Hizir et al., 2014; Lu et al., 2005). Furthermore, miRNAs are accurate clusters for different types of solid tumors and the fold change in miRNAs between cancer cells and normal cells is relatively large (Zhang et al., 2014). Therefore, it is urgently needed to detect miRNAs for early diagnosis and pathogenesis of cancers. Some bioanalytical methods have been developed to identify and quantify miRNA, such as Northern blotting (Várallyay et al., 2008), microarrays (Castoldi et al., 2008), and real-time polymerase chain reaction (PCR) (Li et al., 2009; Yu et al., 2013). However, the intrinsic characteristics of miRNA, including its short size, sequence homology among family members, low abundance in total RNA samples, and susceptibility to degradation, impose great challenges in the analysis using these methods. (Li et al., 2015b; Yin et al., 2013)

By combining with some amplification strategies, various biosensors have been

developed and applied to miRNA analysis (Bi et al., 2013; Chen et al., 2015; Cissell et al., 2008; Ding et al., 2015; Li et al., 2015a; Yu et al., 2014; Zheng et al.,2015). Among these methods, SPR biosensor, which monitors the change in refractive index near the surface that occurs during complex formation or dissociation, is an attractive technology for sensitive, label-free, and real-time detection of biomolecular targets (Liu and Cheng, 2012; Zagorodko et al., 2014). Generally, some amplification strategies, including biomolecules enhancement (Ding et al., 2015; Nasheri et al., 2011; Sípová et al., 2010; Zhang et al., 2013a) and nanoparticle enhancement (Fang et al., 2006; Zhou et al., 2011), have been developed for improving the sensitivity of SPR biosensor to miRNA. Nevertheless, a number of constraints associated with biomolecules still exist, such as limited stability, difficulties in storage, and the high cost. In particular, the methods that involved enzymatic modification of the target miRNA were expensive and need special reaction conditions (Fang et al., 2006; Zhou et al., 2011). Thus, the development of nanomaterial-based amplification strategies would facilitate the monitoring of miRNA, because of their advantages such as low cost, high stability and tunability in comparison with biomolecular.

Various nanomaterials have been used in SPR analysis of biomolecules (Zeng et al., 2014), such as metal nanoparticles (Hu et al., 2014; Paul et al., 2011; Vaisocherova et al., 2015; Wang et al., 2016), magnetic nanoparticles (Wang et al., 2010), SiO_2 nanoparticles (Zhou et al., 2011), quantum dots (Vance and Sandros, 2014), carbon nanotube (Lee et al., 2011). In view that the graphene oxide-gold nanoparticles (GO-AuNPs) hybrids can increase the available surface area for analyte

binding as well as improve their electrical conductivity and electron mobility, they have hold the greatest promise for implementation into a wide array of biosensors (Cheng et al., 2015; Hu et al., 2015; Li et al., 2015c; Yuan et al., 2013). Recently, the GO-AuNPs hybrids have been applied in the SPR biosensors for the detection of ractopamine (Yao et al., 2016) and IgG (Zhang et al., 2013b). The GO-AuNPs hybrids were used as a solid support for the immobilization of recognition molecules in these previous works. However, few papers have reported on the utilization of GO-AuNPs hybrids, which played as signal tags, for the sensitive detection of miRNA.

Herein, a novel and simple GO-AuNPs hybrids-based SPR biosensor (GOAu-SPR) was designed for the detection of miRNAs. As a proof of concept, miRNA-141, which showed overexpression in the prostate cancer, was chose as a model target miRNA. DNA-linked GO-AuNPs hybrids were used as signal tags and to form a sandwich complex on the SPR sensing surface. On the one hand, the SPR signal was enhanced by the electronic coupling between localized plasmon of AuNPs and the surface plasmon wave associated with Au film (He et al., 2000; Liu and Cheng, 2012; Wang et al., 2011). On the other hand, GO possessed large specific surface area and loaded a large amount of AuNPs, so the SPR signal could be further enhanced. With the amplification of GO-AuNPs hybrids, a detection limit of as low as 1 fM for miRNA-141 was achieved. Moreover, this method also demonstrated high selectivity for discriminating differences between miRNA family members and good performance in a complex biological matrix. Meanwhile, since the single stranded state of thiolated DNA can be regenerated simply, this biosensor possessed the

property of reproducibility. Comparing with the standard bioanalytical methods, which were often expensive, complicated, and need highly trained technicians, the GOAu-SPR was performed in only two simple steps and cost-effective.

2. Experimental

2.1. Chemicals and materials

Chloroauric acid ($HAuCl_4 \cdot 4H_2O$) and trisodium citrate were purchased from Shanghai Reagent Company (Shanghai, China). 6-Mercapto-1-hexanol (MCH) was purchased from Sigma (USA). The DNA sequences were synthesized by Shanghai Sangon Biotechnology Co. (Shanghai, China). The RNA sequences were synthesized by TaKaRa Biotechnology Co. (Dalian, China). The sequences of DNA and RNA were listed in **Table 1**. Other reagents used in the experiments were of analytical grade or higher. Ultrapure water (18.2 MΩ·cm) was used throughout. Capture DNA and miRNA-141 were dissolved into 10 mM PBS buffer (pH 7.4) containing 100 mM NaCl before use. All of the solutions used were treated with diethylpyrocarbonatex (DEPC) and autoclaved to protect from RNase degradation. The AuNPs (18 ± 2) were prepared by the citrate reduction of $HAuCl_4$ following a literature procedure (Grabar et al., 1995).

Table 1. positioned here

2.2. Apparatus

The transmission electron microscopic (TEM) images were obtained on Tecnai 20 transmission electron microscope (FEI., USA). The scanning electron microscope (SEM) images were obtained on a MIRA3 scanning electron microscope (TESCAN,

Czech). The X-ray photoelectron spectroscopy (XPS) measurements were investigated using monochromatized Al-Kα (1486.6 eV) X-ray source in Thermo ESCALAB 250XI apparatus (Thermo Fisher, USA). The UV-vis absorption spectra were obtained with Biospec-nano UV-vis spectrophotometer (Shimadzu, Japan). All SPR measurements were performed with EC-SPR1010 device (Changchun Dingcheng Technology, China).

2.3. Preparation and modification of GO-AuNPs hybrids

The GO-AuNPs hybrids were prepared by the reduction of gold (III) complex with sodium citrate (Goncalves et al., 2009). Typically, 25 mL of 0.48 mM $HAuCl_4$ solution was mixed with 1.25 mL of 1 mg mL^{-1} GO solution. After the mixture was aged for 30 min at room temperature, the solution was heated to 80 °C. Then 470 μL of 85 mM sodium citrate was added dropwise. After incubation for 60 min, the mixture was centrifuged (15min, 5000 rpm), and the resultant composite was washed with distilled water to remove the free gold nanoparticles that formed in solution.

DNA-linked GO-AuNPs hybrids were prepared according to the literature with minor modifications (Wang et al., 2011). Assistant DNA (9 μL, 100 μM) and helper DNA (9 μL, 100 μM) were first mixed with 882 μL GO-AuNPs hybrids solution for 16 h at 4 °C, then the solution was brought to 100 mM NaCl solution (pH 7.0, 10 mM phosphate buffer) for aging 40 h at 4 °C. Next, the DNA-linked GO-AuNPs hybrids were centrifuged (20 min, 13500 rpm) to remove excess reagents. The supernatant was discarded and the precipitate was washed with 100 mM NaCl solution (pH 7.0, 10 mM PBS). After a second centrifugation, the precipitate was dispersed in 600 μL,

100 mM NaCl solution (pH 7.0, 10 mM PBS).

2.4. Surface modification of Au film

Au film was first cleaned in acetone, ethanol and water for 2 min in each solution. Then the Au film was cleaned with fresh piranha solution (98% H_2SO_4/H_2O_2, 7:3 (v/v)) followed by a thorough rinsing with water. DNA-modified surfaces were prepared by incubation of Au film with 5 μM capture DNA in 10 mM PBS (pH 7.4) for 2 h incubation. Then, Au film was rinsed with 10 mM PBS (pH 7.4) thoroughly. Subsequently, Au film surface was passivated with 1 mM MCH for 30 min at room temperature in order to reduce nonspecific binding of DNA on the Au film surface. In addition, thiol-modified capture DNA molecules were also raised off the surface by MCH (Herne and Tarlov, 2008). After thoroughly rinsing with 10 mM PBS (pH 7.4), the sensor chip was obtained.

2.5. miRNA detection protocol

Detection of miRNA-141 was conducted by exposing the sensor chip to different concentration of miRNA-141 solution or tumor cell extractions for 50 min at room temperature, then washing with 10 mM PBS repeatedly. The resonance angle was recorded. Next, DNA-linked GO-AuNPs hybrids were added for reacting about 60min at room temperature. After washing with 10 mM PBS repeatedly, the resonance angle was recorded. 0.1% SDS/10 mM NaOH was introduced for 5 min to regenerate the sensor chip for further use.

2.6. Cell extractions and qRT-PCR analysis

The total RNA, including miRNA, was extracted from human cancer cell lines

using Trizol reagent (Sangon Co. Ltd., Shanghai, China) according to the manufacturer's instructions. The pure and concentrated RNA was then divided into two equal parts for detection using the GOAu-SPR assay and qRT-PCR.

The cDNA samples were prepared by using the reverse transcription (RT) reaction with AMV First Strand cDNA Synthesis Kit (BBI, Toronto, Canada). The transcribed cDNA was then used as the template for qRT-PCR. qPCR analysis of miRNA was performed with SG Fast qPCR Master Mix(2X) (BBI), according to the indicated protocol on an LightCycler480 Software Setup (Roche).

3. Results and discussion

3.1. Principle of the GOAu-SPR biosensor

The procedure for the GOAu-SPR biosensor was showed in **Fig. 1.** The assay was performed in two simple steps. In the first step, the Au film surface functionalized with covalently attached thiolated DNA probes, having sequence complementary to the targeted miRNA, was incubated with the sample containing miRNA. In this step, the miRNA was captured by the DNA probes. In the second step, the Au film surface was incubated with DNA-linked GO-AuNPs hybrids that specifically bound to the surface by hybridization with terminus of capture DNA.

Fig. 1. positioned here

3.2 Characterization of GO-AuNPs hybrids

The synthesized GO-AuNPs hybrids were characterized using TEM. As shown in **Fig. 2A**, a distribution of Au nanoparticles with diameters of 18 ± 2 nm was observed at the GO surface.

UV-visible absorption spectra were used for optical characterization of GO-AuNPs hybrids and DNA-linked GO-AuNPs hybrids in solution. The absorption spectrum of GO-AuNPs hybrids showed two peaks at about 230.0 and 524.0 nm (**Fig. 2B,** curve a), which corresponded to the characteristic absorption of GO and AuNPs, respectively, indicating the successful assembly of AuNPs on GO. This result was consistent with that of TEM image (**Fig. 2A**). In addition, GO-AuNPs hybrids were modified with assistant DNA, and the absorption spectrum of DNA-linked GO-AuNPs hybrids was shown in **Fig. 2B**. On the absorption spectra of GO-AuNPs hybrids and DNA-linked GO-AuNPs hybrids, the characteristic absorption peak of AuNPs was 524.0 nm (**Fig. 2B,** curve a) and 528.0 nm (**Fig. 2B,** curve b), respectively, confirming that GO-AuNPs hybrids was labeled with assistant DNA.

Fig. 2. positioned here

3.3. Characterization of the feasibility

The feasibility of this method was first investigated. As shown in **Fig. 3**, as 50 pM target miRNA-141 was added and incubated with capture DNA coated Au film, SPR spectrum shifted from curve 1 to curve 2 and small resonance angle shift (0.0048^{o}) was observed. Then DNA-linked GO-AuNPs hybrids were added, SPR spectrum shifted from curve 2 to curve 3 and an obvious resonance angle shift (0.2130^{o}) was observed, suggesting that the DNA-linked GO-AuNPs hybrids were captured on the Au film through hybridization. Due to the electromagnetic coupling between the AuNPs and the underlying Au film, and the high mass-density and dielectric constant of the AuNPs on the surface of GO sheets, a striking signal enhancement was induced.

When 0.1% SDS/10 mM NaOH was introduced for 10 min, SPR spectrum shifted from curve 3 to curve 4. The resonance angle of curve 4 was basically consistent with that of curve 1, implying that the sensor chip could be regenerated.

Fig. 3. positioned here

In addition, the feasibility of this method was also characterized using SEM. When 50 pM miRNA-141 was presented, it was found that GO-AuNPs hybrids distributed on the Au film (**Fig. 4A**), while few nanoparticles could be observed in the absence of miRNA-141 (**Fig. 4C**). The amount of the GO-AuNPs hybrids increased as the miRNA-141 concentration increased (**Fig. 4**). The results demonstrated that the as-designed SPR biosensor can be used for miRNA detection.

Fig.4. positioned here

Surface characterization of the Au film at each stage of experiment was conducted using X-ray photoelectron spectroscopy (XPS). **Fig. 5A** showed XPS spectra of N1s for bare Au film and capture DNA modified Au film, respectively. Compared with the N1s spectrum of bare Au film (curve a of **Fig. 5A**), the N1s spectrum of capture DNA modified Au film (curve b of **Fig. 5A**) showed an increased intensity of N element, implying that capture DNA was effectively assembled on the Au film. **Fig. 5B** showed the XPS spectra of C1s for bare Au film (curve a), capture DNA modified Au film (curve b) and assistant DNA-linked GO-AuNPs hybrids modified Au film (curve c). As shown in **Fig. 5B**, the main peak of C1s spectrum related to C−C/C=C (284.8 eV) appeared. As the Au film was modified with capture DNA, a peak emerged at 286.4 eV (curve b of **Fig. 5B**), which was associated with

the C-O bond in DNA. In the presence of target miRNA, the assistant DNA-linked GO-AuNPs hybrids were added, and a peak appeared at 288.7 eV (curve c of **Fig. 5B**), which was corresponded to the O-C=O bond of GO. The results showed that the capture DNA and the assistant DNA-linked GO-AuNPs hybrids were assembled on the Au film successfully.

Fig.5. positioned here

3.4. Analytical performance of miRNA-141 detection

Different concentrations of miRNA-141 were detected. **Fig. 6A** showed the resonance angle gradually increased as the miRNA-141 concentration increased from 0 to 50 pM, due to the increased quantity of DNA-linked GO-AuNPs hybrids which were captured on Au film. **Fig. 6B** showed the relation between $\Delta\theta$ and the concentration of miRNA-141 of three methods (i.e. direct hybridization measurement, AuNPs amplified SPR and GOAu-SPR). Since a shift of resonance angle larger than 0.0015^{o} was regarded as signal for the SPR instrument, it was estimated that the detection limit of direct hybridization measurement, AuNPs amplified SPR and GOAu-SPR were *ca.*100 pM (curve a of **Fig. 6B**), 1 pM (curve b of **Fig. 6B**) and 1fM (curve c of **Fig. 6B**), respectively. In other words, the detection limit of GOAu-SPR was 3 order of magnitude lower than that of AuNPs amplified SPR and 5 order of magnitude lower than that of direct hybridization measurement. Moreover, a comparison between the present work and previously reported studies was performed. As shown in **Table 2**, the sensitivity of this sensor was comparable to or better than that of those previous works. The results showed the high amplification efficiency of

the GOAu-SPR biosensor.

Fig. 6. positioned here

Table 2. positioned here

Distinguishing among members from the same miRNA family is of great importance for better understanding the biological functions of individual miRNAs. Since miRNA families often possess closely related sequences with high homology, it is a great challenge to discriminate the differences between miRNA family members. To evaluate the specificity of the GOAu-SPR biosensor, miRNA-141, miRNA-429, miRNA-200a, miRNA-21 and random miRNA were used for analysis. Among them, miRNA-141, miRNA-429 and miRNA-200a belong to the miRNA-200 family. miRNA-21 is reported as an antiapoptotic factor in cancer cells and shows overexpression in various cancers. As expected, there was no change in angle shift in the case of miRNA-21 and random miRNA (**Fig. 6C**). For miRNA-429 and miRNA-200a, $\Delta\theta$ increased slightly as the concentrations of miRNA-429 and miRNA-200a were increased; while $\Delta\theta$ increased obviously as the increase of miRNA-141 concentration. Take 10 pM miRNA as example, $\Delta\theta$ was 0.1651^{o} for miRNA-141, which was more than eight times larger than that of miRNA-429 and five times larger than that of miRNA-200a. The results clearly demonstrated that this biosensor had high sequence specificity to distinguish among miRNA family members, which further supported the feasibility of the proposed method.

The reproducibility of the sensor chip was also investigated. After a sample was detected, the Au film surface was regenerated using 0.1% SDS/10 mM NaOH for the

next round of analysis. When the GOAu-SPR biosensor was used to detect 10 pM miRNA-141, no significant signal degradation was observed during the 5 cycles and the standard deviation was less than 1% (**Fig. 6D**), implying that this SPR biosensor exhibited good reproducibility.

3.5. Application of the biosensor in cell extractions

To investigate the capacity of the GOAu-SPR biosensor for detection of cancer cell extractions, four human cancer cell lines, including prostate carcinoma cell lines (22Rv1), hepatocellular carcinoma cell lines (SMMC-7721), colon cancer cell lines (LoVo), and cervical cancer cell lines (HeLa), were chosen to measure the expression of miRNA-141 in total RNA from cells lines. The relative expression levels based on the expression ratio of miRNA-141 in target cell lines versus that in 22Rv1 cell lines were used to characterize miRNA-141 levels. Herein the relative expression levels of miRNA-141 in total RNA were specifically determined using qRT-PCR and the GOAu-SPR biosensor. As shown in **Fig. 7**, the developed SPR biosensor generated a result similar to that of qRT-PCR. Both of the methods showed that miRNA-141 had different expression levels in four cancer cell lines. It was observed that the cell extractions from prostate carcinoma 22Rv1 cells lines and colon cancer LoVo cell lines had a higher concentration of miRNA-141 than that of other cells. For example, about 93% decrease in the concentration of miRNA-141 was observed in 7721 cells compared to 22Rv1 cells, which was comparable with that (about 95% decrease) obtained from the qRT-PCR detection. Meanwhile, this result was in good accordance with reported literature that miRNA-141 expresses in a wide range of common human

cancers including colon, and prostate cancer (Yin et al., 2012). The overall results indicated that this SPR biosensor holds a great promise for practical applications in miRNA detection with great reliability.

Fig. 7. positioned here

4. Conclusion

In summary, a novel and simple GO-AuNPs hybrids-based SPR biosensor (GOAu-SPR) for miRNA detection was developed, in which GO-AuNPs hybrids were used as signal-enhancing label. The GOAu-SPR showed superior sensitivity and excellent selectivity for discriminating among miRNA family members. For the detection of miRNA-141 in cell extractions, the results obtained using the GOAu-SPR biosensor were in excellent agreement with the ones obtained using qRT-PCR. In contrast to the existing methods for miRNA detection, the GOAu-SPR biosensor eliminated the need for special capture probe (e.g. LNA probe), and the use of an expensive kit or of toxic chemicals. On the basis of the distinctive properties, the GOAu-SPR biosensor was suitable for serving as a promising tool in clinical application. However, this GOAu-SPR biosensor was comparatively time-consuming. For prospective development, it is worthwhile to attempt to improve the sample injection system based on the microfluidics for shortening the detection time.

Acknowledgments

This work was supported by the National Natural Science Foundation of China (21190040, 21375034 and 21175035), National Basic Research Program (2011CB911002), International Science & Technology Cooperation Program of China (2010DFB30300), and the Fundamental Research Funds for the Central Universities of China.

References

Bi, S., Cui, Y.Y., Li, L., 2013. Anal. Chim. Acta. 760, 69–74.

Calin, G. A., Croce, C. M., 2006. Nat. Rev. Cancer 6, 857–866.

Castoldi, M., Schmidt, S., Benes, V., Hentze, M.W., Muckenthaler, M.U., 2008. Nat. Protoc. 3, 321–329.

Chen, A.Y., Gui, G.F., Zhuo, Y., Chai, Y.Q., Xiang, Y., Yuan, R., 2015. Anal. Chem. 87, 6328–6334.

Cheng, F.F., He, T.T., Miao, H.T., Shi, J.J., Jiang, L.P., Zhu, J.J., 2015. ACS Appl. Mater. Interfaces 7, 2979–2985.

Cissell, K.A., Rahimi, Y., Shrestha, S., Hunt. E.A., Deo, S.K., 2008. Anal. Chem. 80, 2319–2325.

Ding, X.J., Yan, Y.R., Li, S.Q., Zhang, Y., Cheng, W., Cheng, Q., Ding, S.J., 2015. Anal. Chim. Acta. 874, 59–65.

Fang, S.P., Lee, H.J., Wark, A.W., Corn, R.M., 2006. J. Am. Chem. Soc. 128, 14044–14046.

Goncalves, G., Marques, P. A. A. P., Granadeiro, C. M., Nogueira, H. I. S., Singh, M. K., Gracio, J., 2009. Chem. Mater. 21, 4796–4802.

Grabar, K.C., Freeman, R.G., Hommer, M.B., Natan, M.J., 1995. Anal. Chem. 67, 735–743.

He, L., Hannon, G., 2004. Nat. Rev. Genet. 5, 522–531.

He, L., Musick, M.D., Nicewarner, S.R., Salinas, F.G., Benkovic, S.J., Natan, M.J., Keating, C.D., 2000. J. Am. Chem. Soc. 122, 9071–9077.

Herne, T.M., Tarlov, M.J., 1997. J. Am. Chem. Soc. 119, 8916–8920.

Hizir, M.S., Balcioglu, M., Rana, M., Robertson, N.M., Yigit, M.V., 2014. ACS Appl. Mater. Interfaces 6, 14772–14778.

Hu, W.H., He, G.L., Zhang, H.H, Wu, X.S., Li, J.L., Zhao, Z.L., Qiao, Y., Lu, Z.S., Liu, Y., Li, C.M., 2014. Anal. Chem. 86, 4488–4493.

Lee, E.G., Park, K.M., Jeong, J.Y., Lee, S.H., Baek, J.E., Lee, H.W., Jung, J.K., Chung, B.H., 2011. Anal. Biochem. 408, 206–211.

Li, F.Y., Peng, J., Zheng, Q., Guo, X., Tang, H., Yao, S.J, 2015a. Anal. Chem. 87, 4806–4813.

Li, J., Yao, B., Huang, H., Wang, Z., Sun, C.H., Fan, Y., Chang, Q., Li, S.L., Wang, X., Xi, J.Z., 2009. Anal. Chem. 81, 5446–5451.

Li, W., Jiang, W., Ding, Y.S., Wang, L., 2015b. Biosens. Bioelectron. 71, 401–406.

Li, Y., Deng, J., Fang, L.C., Yu, K.K., Huang, H., Jiang, L.L., Liang, W.B., Zheng, J.S., 2015c. Biosens. Bioelectron. 63, 1–6.

Liu, Y., Cheng, Q., 2012. Anal. Chem. 84, 3179–3186.

Lu, J., Getz, G., Miska, E. A., Alvarez-Saavedra, E., Lamb, J., Peck, D., Sweet-Cordero, A., Ebert, B. L., Mak, R. H., Ferrando, A. A., Downing, J. R., Jacks, T., Horvitz, H. R., Golub, T. R., 2005. Nature 435, 834–838.

Nasheri, N., Cheng, J., Singaravelu, R., Wu, P., McDermott, M.T., Pezacki, J.P., 2011. Anal. Biochem. 412, 165–172.

Paul, S., Paul, D., Fern, G.R., Ray, A.K., 2011. J. R. Soc. Interface 8, 1204–1211.

Sípová, H., Zhang, S., Dudley, A.M., Galas, D., Wang, K., Homola, J., 2010. Anal. Chem. 82, 10110–10115.

Várallyay, E., Burgyán, J., Havelda, Z., 2008. Nat. Protoc. 3, 190–196.

Vance, S.A., Sandros, M.G., 2014. Sci. Rep. 4, 5129–5135.

Vaisocherova, H., Sipova, H., Visova, I., Bockova, M., Springer, T., Ermini, M.L., Song, X., Krejcik, Z., Chrastinova, L., Pastva, O., 2015. Biosens. Bioelectron. 70, 226–231.

Wang, J.L., Munir, A., Zhu, Z.Z., Zhou, H.S., 2010. Anal. Chem. 82, 6782–6789.

Wang, Q., Huang, J.H., Yang, X.H., Wang, K.M., He, L.L., Li, X.P., Xue, C.Y., 2011a. Sensor Actuat. B 156, 893-898.

Wang, Q., Yang, L.J., Yang, X.H., Wang, K.M., He, L.L., Zhu, H.Z., 2011b. Anal. Chim. Acta. 688, 163-167.

Wang, Q., Liu, R.J., Yang, X.H., Wang, K.M., Zhu, J.Q., He, L.L., Li, Q., 2016. Sensor Actuat. B 223, 613–620.

Yao, T., Gu, X., Li, T.F., Li, J.G., Li, J., Zhao, Z., Wang, J., Qin, Y.C., She, Y.X., 2016. Biosens. Bioelectron. 75, 96–100.

Yin, B.C., Liu, Y.Q., Ye, B.C., 2012. J. Am. Chem. Soc. 134, 5064–5067.

Yin, B.C., Liu, Y.Q., Ye, B.C., 2013. Anal. Chem. 85, 11487–11493.

Yuan, Y.L., Liu, G.P., Yuan, R., Chai, Y.P., Gan, X.X., Bai, L.J., 2013. Biosens. Bioelectron. 42, 474–480.

Yu, C.Y., Yin, B.C., Ye, B.C., 2013. Chem. Commun. 49, 8247–8249.

Yu, Y.Y., Chen, Z.G., Shi, L.J., Yang, F., Pan, J.B., Zhang, B.B., Sun, D.P., 2014. Anal. Chem. 86, 8200–8205.

Zagorodko, O., Spadavecchia, J., Serrano, A.Y., Larroulet, I., Pesquera, A., Zurutuza,

A., Boukherroub, R., Szunerits, S., 2014. Anal. Chem. 86, 11211–11216.

Zeng, S.W., Baillargeat, D., Ho, H.P., Yong, K.T., 2014. Chem. Soc. Rev. 43, 3426–3452.

Zhang, X., Wu, D.Z., Liu, Z.J., Cai, S.X., Zhao, Y.P., Chen, M., Xia, Y.K., Li, C.Y., Zhang, J., Chen, J.H., 2014. Chem. Commun. 50, 12375–12377.

Zhang, D.C., Yan, Y.R., Cheng, W., Zhang, W., Li, Y.H., Ju, H.X., Ding, S.J., 2013a. Microchim. Acta 180, 397–403.

Zhang, J., Sun, Y., Wu, Q., Zhang, H., Bai, Y., Song, D.Q., 2013b. Analyst 138, 7175 – 7181.

Zheng, J., Bai, J.H., Zhou, Q.H., Li, J.S., Li, Y.H., Yang, J.F., Yang, R.H., 2015. Chem. Commun. 51, 6552–6555.

Zhou, W.J., Chen, Y.L., Corn, R.M., 2011. Anal. Chem. 83, 3897–3902.

Table caption

Table 1. Sequences of DNA probes used.

Table 2. Detection performance comparison of our strategy with other SPR methods

Figures Caption

Fig. 1. The schematic illustration of the SPR biosensor based on the GO-AuNPs hybrids amplification.

Fig. 2. (A) TEM image of GO-AuNPs hybrids; (B) UV-Vis adsorption spectra of GO-AuNPs hybrids (a) and DNA-linked GO-AuNPs hybrids (b).

Fig. 3. SPR spectra of (1) capture DNA modified Au film; (2) hybridization with 50 pM miRNA-141; (3) reaction with the DNA-linked GO-AuNPs; (4) regeneration.

Fig. 4. SEM images of Au film in the presence of miRNA-141. (A) 50 pM; (B) 10pM and (C) 0 pM. Scale bar: 500 nm.

Fig. 5. (A) The N1s XPS spectra of bare Au film (curve a) and capture DNA modified Au film (curve b); (B) The C1s XPS spectra of bare Au film (curve a), capture DNA modified Au film (curve b) and assistant DNA-linked GO-AuNPs hybrids modified Au film (curve c).

Fig. 6. (A) SPR spectra of different concentrations of miRNA-141. (B) The relationship between $\Delta\theta$ and miRNA-141 concentrations by using different sensing strategies. Error bars showed the standard deviation of measurement taken from three experiments. (a) direct hybridization measurement, (b) AuNPs amplified SPR, and (c) GOAu-SPR. (C) Selectivity investigation of the GOAu-SPR biosensor. (D) Reproducibility investigation of the GOAu-SPR biosensor. The sensor chip was regenerated by introducing 0.1% SDS / 10 mM NaOH for 5 min.

Fig. 7. Paired comparison of the miRNA-141 levels detected in total RNA isolated from four kinds of human cancer cell lines using the GOAu-SPR biosensor (blue histogram) or qRT-PCR (pink histogram). Relative signal intensity was based on the expression ratio of miRNA-141 in target cell lines versus that in 22Rv1 cell lines. Error bars showed the standard deviation of measurement taken from three experiments. The repeatability of the biosensor was evaluated from the relative standard deviation (RSD) of four cell lines. The RSD values were $\leq$ 5% for the GOAu-SPR biosensor and $\leq$ 12% for qRT-PCR.

Table 1. Sequences of DNA probes used

Name	Sequence (5'-3')
Capture DNA	AGA CAG TGT TAT TTT TTT TTT-SH
Assistant DNA	SH-TTT TTT TTT TTT TCC ATC TTT ACC
Helper DNA	SH-TTT TTT TTT TTT T
miRNA-141	UAACACUGUCUGGUAAAGAUGG
miRNA-429	UAAUACUGUCUGGUAAAACCGU
miRNA-200a	UAACACUGUCUGGUAACGAUGU
miRNA-21	UAGCUUAUCAGACUGAUGUUGA
Radom miRNA	N_{22}

Table 2. Detection performance comparison of our strategy with other SPR methods.

SPR platform	Amplification strategy	Detection limit	Reference
Biacore X	Streptavidin complex amplification	17 pM	Zhang et al., 2013
Biacore X	Streptavidin and supersandwich amplification	9 pM	Ding et al., 2015
SPRCD	Antibody amplification	2 pM	Sípová et al., 2010
SPR imaging	Protein p19 amplification	1 fM	Nasheri et al., 2011
SPR imaging	AuNPs amplification	0.5 pM	Vaisocherova et al., 2015
SPRimager	AuNPs and polymerase amplification	10 fM	Fang et al., 2006
SPRimager	Silica nanoparticles and polymerase amplification	100 fM	Zhou et al., 2011
SPR	AuNPs and DNA supersandwich amplification	8 fM	Wang et al., 2016
GOAu-SPR	GO-AuNPs hybrids amplification	1 fM	This work

Highlight

A simple SPR biosensor for sensitive and selective detection of miRNA was introduced.

The GO-AuNPs hybrids were used as signal tags to enhance the SPR signal.

It can be used for miRNA detection in cancer cell extractions.

This assay has great promise for biomedical research and early clinical diagnostics.

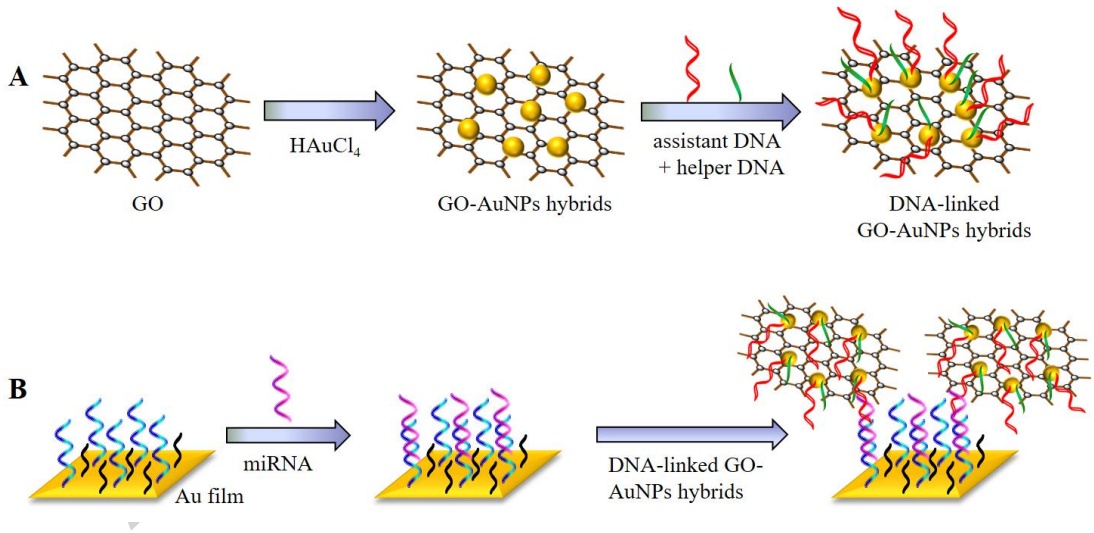

Fig. 1. The schematic illustration of the SPR biosensor based on the GO-AuNPs hybrids amplification.

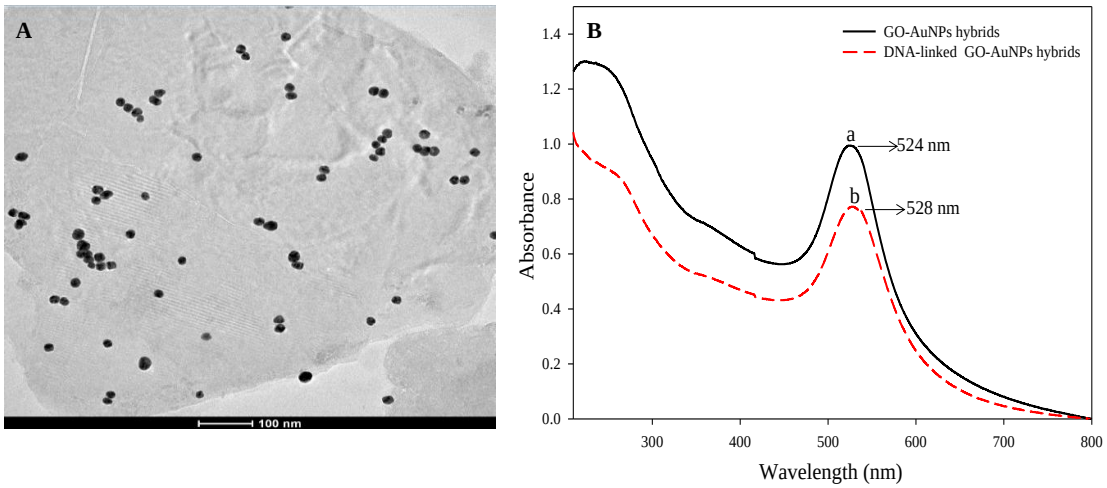

Fig. 2. (A) TEM image of GO-AuNPs hybrids; (B) UV-Vis adsorption spectra of GO-AuNPs hybrids (a) and DNA-linked GO-AuNPs hybrids (b).

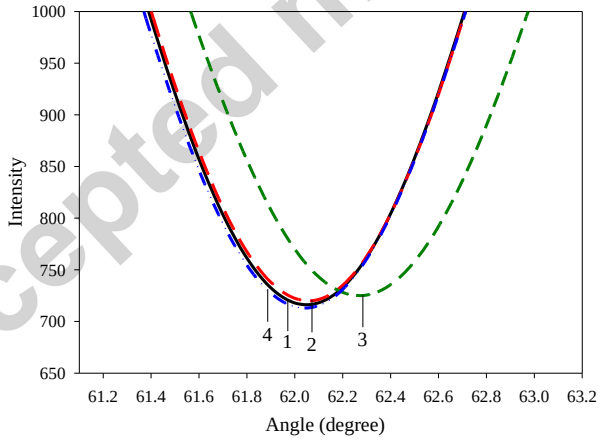

Fig. 3. SPR spectra of (1) capture DNA modified Au film; (2) hybridization with 50 pM miRNA-141; (3) reaction with the DNA-linked GO-AuNPs; (4) regeneration.

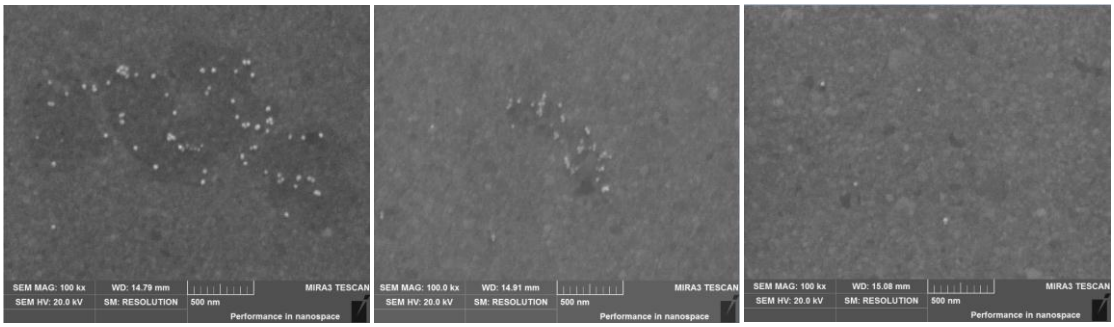

Fig. 4. SEM images of Au film in the presence of miRNA-141. (A) 50 pM; (B) 10pM and (C) 0 pM. Scale bar: 500 nm.

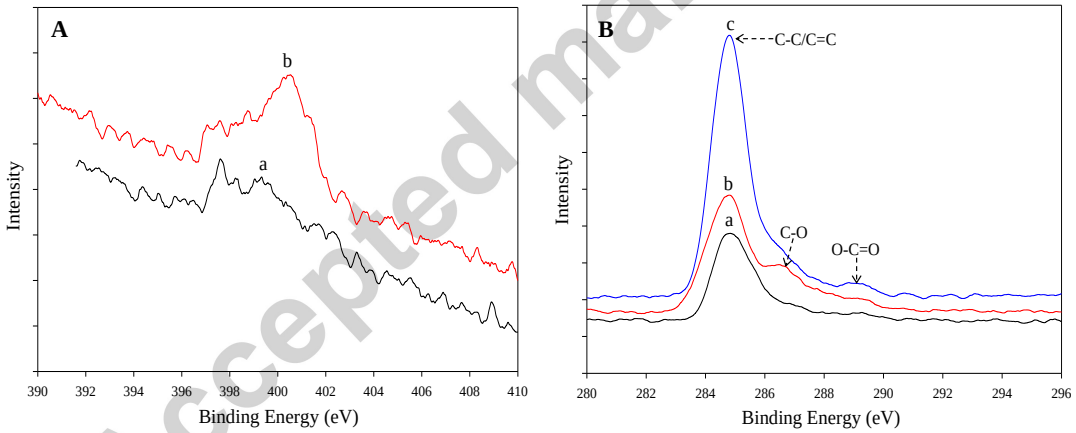

Fig. 5. (A) The N1s XPS spectra of bare Au film (curve a) and capture DNA modified Au film (curve b); (B) The C1s XPS spectra of bare Au film (curve a), capture DNA modified Au film (curve b) and assistant DNA-linked GO-AuNPs hybrids modified Au film (curve c).

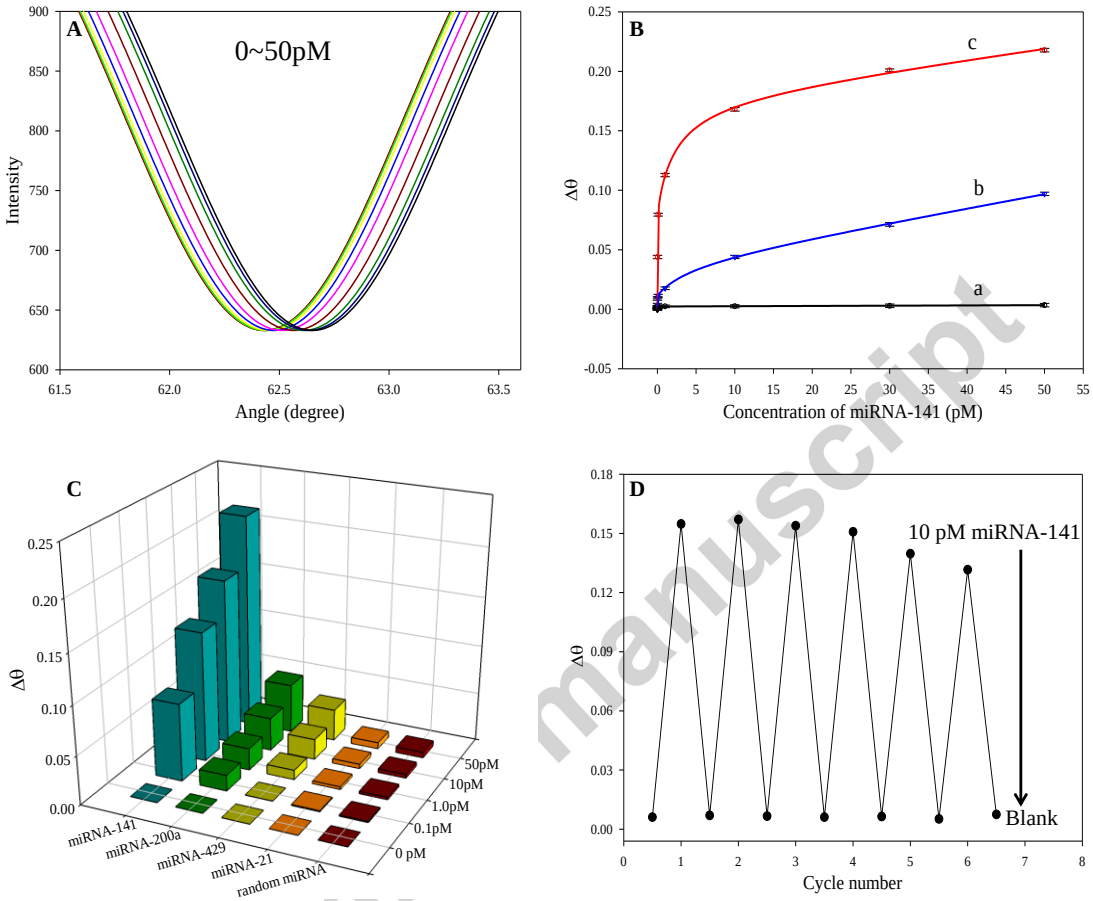

Fig. 6. (A) SPR spectra of different concentrations of miRNA-141. (B) The relationship between Δθ and miRNA-141 concentrations by using different sensing strategies. Error bars showed the standard deviation of measurement taken from three experiments. (a) direct hybridization measurement, (b) AuNPs amplified SPR, and (c) GOAu-SPR. (C) Selectivity investigation of the GOAu-SPR biosensor. (D) Reproducibility investigation of the GOAu-SPR biosensor. The sensor chip was regenerated by introducing 0.1% SDS / 10 mM NaOH for 5 min.

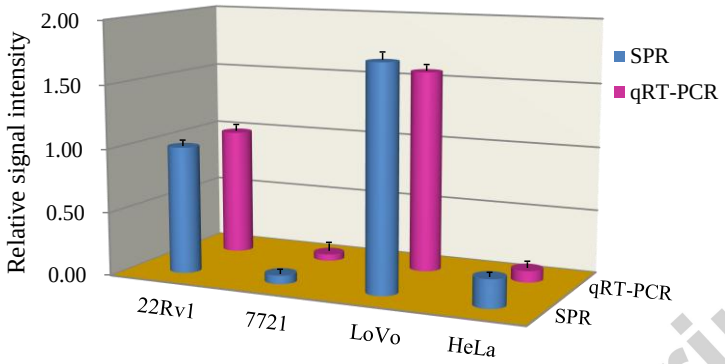

Fig. 7. Paired comparison of the miRNA-141 levels detected in total RNA isolated from four kinds of human cancer cell lines using the GOAu-SPR biosensor (blue histogram) or qRT-PCR (pink histogram). Relative signal intensity was based on the expression ratio of miRNA-141 in target cell lines versus that in 22Rv1 cell lines. Error bars showed the standard deviation of measurement taken from three experiments. The repeatability of the biosensor was evaluated from the relative standard deviation (RSD) of four cell lines. The RSD values were ≤ 5% for the GOAu-SPR biosensor and ≤ 12% for qRT-PCR.